# Cleaning Properties of Single-Phase Hydrocarbon-Based Microemulsion Systems

**J. Klier*, R.S. Suarez, D.P. Green, A.M. Kumar, M. Hoffman, C.J. Tucker, B. Landes, and D. Redwine**

The Dow Chemical Company, Midland, Michigan 48674

**ABSTRACT:** Single-phase hydrocarbon-based microemulsions with low volatile organic carbon levels can help deliver solvent-like cleaning properties while allowing formulators to meet regulatory requirements. The rheology and petroleum jelly solubilization properties of model microemulsion systems that contained equal volumes of hydrocarbon solvent and water were evaluated as a function of microemulsion structure and composition. Single-phase microemulsions with low surfactant contents and broad formulation flexibility were obtained through the use of efficient anionic surfactants and low electrolyte levels. The microemulsion structure was advanced from solvent-continuous to water-continuous by varying the solvent alkane carbon number or the electrolyte content, whereas the liquid crystal content was controlled *via* cosurfactant concentration. Both microemulsion structure and viscosity influenced solubilization rates. Low-viscosity, solvent-continuous microemulsions showed solubilization rates comparable to those found with solvent-based systems, while water-continuous microemulsions showed relatively poor solubilization rates. Microemulsions containing dispersed liquid crystals exhibited high viscosity and low solubilization rates.

*JAOCS 74*, 861–867 (1997).

**KEY WORDS:** Characterization, cleaning, cosurfactant, diffusion, liquid crystal, microemulsion, phase behavior, solubilization, solvent, surfactant.

Federal and state regulations are limiting the maximum permitted solvent content of industrial and consumer cleaners. Solvents that fall under regulatory pressure include volatile organic compounds (VOC), suspected ozone-depleting substances, and potentially hazardous air pollutants. These regulations have resulted in a strong demand for solvent substitutes and solvent reduction technologies.

Microemulsions constitute a class of solvent alternatives that potentially meet both regulatory and performance criteria. They are thermodynamically stable, transparent dispersions of water, organic solvents, and surfactants and are generally characterized as solvent-continuous, water-continuous, or bi-continuous (1). However, high surfactant concentrations are usually required to maintain homogeneity and thermodynamic stability. The high surfactant concentrations contribute to visible postevaporation residue, high formulation viscosity, and high cost. In contrast, microemulsions made with low levels of "efficient" surfactants can give acceptably low residue, low viscosity, and excellent cleaning performance.

For example, microemulsions with low surfactant levels, single-phase behavior, low (50%) VOC levels, reduced flammability, no ozone-depleting potential, solvent-like cleaning performance, and low residue upon evaporation have recently been introduced as solvent substitutes for use in cleaning products (2).

This study was designed to quantify the effects of microemulsion structure, composition, and physical properties on cleaning performance. The study involved formulating a series of model microemulsions, characterizing their structures and dispersed liquid crystal content, evaluating physical properties, and determining the model oily soil (petroleum jelly)-cleaning performance. The microemulsions contained equal volumes of water and hydrocarbon solvent, which were rendered compatible by high-molecular-weight alkylbenzene sulfonate surfactant and diethylene glycol monohexyl ether cosurfactant. The surfactant was chosen based on its ability to stabilize water/hydrocarbon microemulsions at low surfactant concentrations, while the cosurfactant was chosen for its high interfacial activity. This combination of surfactant and cosurfactant facilitates microemulsification of equal volumes of water and hydrocarbon at surfactant concentrations as low as 0.5 wt% in the range of hydrocarbon alkane carbon numbers ($C_6$–$C_{12}$) of interest. As a result of this high microemulsification efficiency, single-phase microemulsions spanning a broad range of structures (solvent to water-continuous) at surfactant concentrations less than 5% surfactant can be formulated. These microemulsions therefore represent attractive model systems for investigating solubilization performance of single-phase microemulsions vs. microemulsion structure and composition, without the problems of phase separation into conjugate phase systems.

## EXPERIMENTAL PROCEDURES

*Surfactant preparation and analysis.* The surfactants used in this study were $C_{20}$–$C_{24}$ linear alkylbenzene sulfonate (ABS). A commercial alkylbenzene, AL-304 alkylbenzene (Chevron,

*To whom correspondence should be addressed. E-mail: jklier@dow.com.

Houston, TX), was distilled to give the $C_{20}$–$C_{24}$ fraction of monoalkylbenzene, which was subsequently sulfonated to ABS with chlorosulfonic acid in the following manner: Alkylbenzene and methylene chloride (1:4, vol/vol) were added to a three-necked round-bottomed 1-L flask that was equipped with a stir bar, addition funnel, thermometer, and septum. The flask was purged with nitrogen for 5 min while cooling to 0°C, and one equivalent of chlorosulfonic acid in methylene chloride (1:1, vol/vol) was added dropwise over 1 h while stirring and maintaining a temperature of 0–5°C. Pentane was added, and the surfactant solution was stripped under reduced pressure at room temperature to remove residual HCl and give the sulfonic acid surfactant.

The surfactant was then neutralized and purified by a liquid extraction process. One part surfactant was dissolved in 19 parts of a 1:1 (w/w) isopropanol/water solution. This solution was saturated with 4.3 parts sodium carbonate, shaken, and then heated to 60°C. The solution separated into a top organic phase and an excess aqueous phase. The organic phase was collected, and the isopropanol was removed under vacuum to give the purified surfactant in a sodium salt form.

The surfactant electrolyte levels were characterized by ion chromatography and inorganic carbon analysis. Ion chromatography was conducted on a 0.5 wt% aqueous solution or dispersion filtered through a 0.2-micron filter. The ion chromatography column employed a Dionex (Sunnyvale, CA) AG4A/AS4A anion exchange medium. The eluent was a 0.002 M sodium carbonate, 0.002 M sodium bicarbonate aqueous solution with a flow rate of 2 mL/min. The injection volume was 50 μL, and the detector was a suppressed conductivity type (Dionex anion micromembrane suppressor with 0.020 N sulfuric acid regenerant at 2–3 mL/min).

Inorganic carbon was determined with a Dohrmann (Santa Clara, CA) DC-80 carbon analyzer. A known amount of sample was injected into a reactor, which contained acidified persulfonate reagent. The sample and reagent reacted to form carbon dioxide, which was quantitated by a nondispersive infrared detector. The results were corrected for sample density.

The alkylbenzene and ABS surfactants were analyzed by $^1$H nuclear magnetic resonance (NMR) and gas chromatography (GC). NMR spectra were obtained on a Gemini VXR-300 (Varian, Palo Alto, CA) spectrometer. GC data were obtained on an HP 5890A (Hewlett-Packard, Palo Alto, CA) gas chromatograph, equipped with a 15 m × 32 mm DB-5 (0.25-micron) column while using the following program: 200°C for 4 min, heated at 10°C/min to 325°C, held at 325°C for 10 min.

To analyze the sulfonic acid surfactants by GC, the surfactants were derivatized to the methyl ester form prior to GC analysis. A 20-mg portion of the sulfonic acid was dissolved in 2 mL acetone, and 10 μL of 0.01 M aqueous phosphoric acid was added, followed by 0.1 mL of trimethylsilyldiazomethane in hexane (2.0 M). The solution was allowed to stand for 30 min, and the solvent was evaporated. The remaining oil was redissolved in 10 mL chloroform for injection.

*Microemulsion preparation and characterization.* The microemulsions were prepared by mixing specified levels of surfactant, cosurfactant, and hydrocarbon solvent, followed by sonication and addition of aqueous sodium chloride solution. The cosurfactant was diethylene glycol monohexyl ether (Aldrich, Milwaukee, WI). Water-to-hydrocarbon solvent ratio was 1:1 (vol/vol), and initial compositions contained 15% (wt/vol) cosurfactant and 5% (wt/vol) surfactant. The water (distilled, deionized) contained 0.07 wt% sodium chloride. The hydrocarbon solvents were linear alkanes, with the alkane length expressed as the alkane carbon number (ACN) (for example, an ACN value of 5 corresponds to pentane). Pure linear alkanes (Aldrich) were used for all integer ACN values. Noninteger ACN values (e.g., 9.5 ACN) were obtained by mixing alkanes with adjacent ACN values, and the average ACN value was reported. All surfactant and cosurfactant percentages are expressed on an additive basis and represent the mass of surfactant or cosurfactant divided by the volume of water plus solvent. The microemulsions were equilibrated for at least 1 wk at 20.5°C, and experimental measurements were also conducted at the same temperature. The reference solutions used in cleaning experiments contained the same levels and types of surfactants, cosurfactants and solvents as the corresponding microemulsions, except the water was replaced with an equal volume of solvent.

Electrical conductivity was evaluated with a customized microprobe, designed to fit into a test tube, and a Fisher Scientific (Pittsburgh, PA) conductivity meter (model 096-32-2), which was calibrated with standard electrolyte solutions.

The presence of liquid crystals was qualitatively determined by a simple optical birefringence technique. Microemulsion samples in glass test tubes were placed between crossed optical polarizers and were back-lit with an incandescent lamp. Isotropic microemulsions appeared dark, whereas samples containing liquid crystals transmitted light and gave a "glowing" appearance. The liquid crystal content was determined by centrifugation. Centrifugation was done in an IEC (International Equipment Co., Needham Heights, MA) Centra-8R centrifuge with a 4-swinging-bucket rotor (number 216) at 3400 rpm.

Viscosities were evaluated at a constant shear rate of 25 $s^{-1}$ in a Brookfield (Brookfield Engineering Labs, Inc., Stoughton, MA) DV III viscometer, equipped with a temperature-controlled water jacket. UL and LV 1, 2, and 3 spindles were employed, depending on the viscosity range of each sample. All samples with liquid crystals were shaken for 5 min prior to viscosity measurements. Samples were shaken in a reciprocating shaker at 160 rpm with a 1.5-in maximum excursion distance.

Surface tension and contact angle values were determined with a Cahn (Cahn Instruments, Inc., Cerritos, CA) DCA-312 dynamic contact angle analyzer. A 50-mL beaker, containing 20–30 mL of test sample, was placed on the platform of the instrument, and the substrate was suspended at least 5 mm above the surface of the test sample. The substrate was then immersed 15 mm and receded. The surface tensions were de-

termined from receding force measurements with flamed glass slides.

The water self-diffusion coefficients were measured by a pulsed gradient spin-echo diffusion (PGSE) NMR technique. Experiments were performed on an Omega 600 (Bruker, Billerica, MA) MHz spectrometer with a 5-mm Bruker Triple × imaging probe with proton detection at 599.76 MHz. Gradient pulses were generated by using the X channel of a 3-channel 10-amp Acustar (Bruker) gradient accessory. Gradient pulses were controlled in the same fashion as radiofrequency pulses by using the PSG pulse controller (Bruker). All pulses were nominally rectangular in shape. Data were acquired by using 20-ms echo delays, and a fixed delay after the gradient pulse was used for all experiments. The NMR free induction decays (FID) were processed in the spectrometer. Phase-corrected spectra were quantitated by peak heights relative to the first experiment in a series. Because of the large number of FID, the individual FID were not examined, and the raw data were presented as peak intensities. The peak intensities, fraction of gradient maximum, and nominal gradient maxima were used to calibrate the diffusion constant:

$$\ln A = D \times G\beta + C \qquad [1]$$

where $D$ is the diffusion constant, $A$ is the peak intensity, $G$ is the gradient field in Hz, and $C$ is a constant, which includes damping due to scalar coupling, and:

$$\beta = \delta^2(\Delta - \delta/3) \qquad [2]$$

where $\delta$ is the gradient pulse length and $\Delta$ is the echo delay.

Small-angle X-ray scattering (SAXS) was used to characterize the microemulsion structures. The SAXS data were acquired with a compact Kratky (Anton Paar, Graz, Austria) camera in conjunction with a position-sensitive proportional counter. The X-ray generator was operated at 40 kV and 40 mA, and an X-ray radiation wavelength of 1.5418Å (CuKα) was employed. Samples were loaded into 0.5-mm quartz capillaries, then sealed prior to analysis. The SAXS experiments were performed in vacuum with the sample in a normal beam transmission mode. Data collection times were set at 10 min. No correction was made for background (parasitic) scattering, while the smearing caused by the slit beam geometry was corrected.

*Petroleum jelly solubilization experiments.* Aluminum coupons of 56 × 9 mm were washed with hexane and acetone and allowed to air-dry. After drying, the coupons were weighed and coated by dipping into a 10-mL graduated cylinder filled to 6 mL with a 1:1 (w/w) petroleum jelly/hexane slurry. The coated coupons were then air-dried for 15 min, and placed under vacuum for 1 h. The coupons were then weighed to determine the amount of deposited petroleum jelly. Only coupons coated with 0.048–0.058 g of petroleum jelly were used for cleaning experiments. Each microemulsion was divided into three 2-dram vials, each filled with 7 mL of microemulsion. The coupons were transferred into the vials, and the vials were capped and placed on a Thermolyne

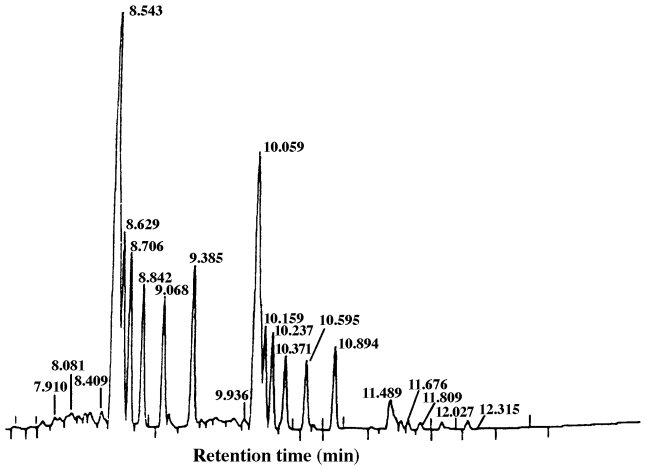


**FIG. 1.** Gas chromatogram of alkylbenzene showing $C_{20}$ benzene at 8.5–9.4 min retention time, $C_{22}$ benzene at 9.8–10.9 min, and $C_{24}$ at 11.4–12.4. The retention time decreases with increasing position of alkyl branching.

Vari-Mix (Barnstead/Thermolyne, Dubuque, IA) rocker at full speed (20 rocks/min.) for 75 s.

After cleaning, the coupons were removed from the vials and tilted to allow a few drops to drip back into the vial. The coupons were then placed into clean, fresh vials, vacuum-dried at 55°C for 24 h, and weighed to determine cleaning. The quantity of nonvolatile residue resulting from evaporation of entrained microemulsion (surfactant, salt, and petroleum jelly) was estimated by using a similar experiment in which a clean coupon was dipped into a "used" microemulsion, dried, and weighed to determine residue levels. The reported "percent clean" values were reduced by the amount of entrained residue. At most, the residue was about 7% of the total amount of petroleum jelly on the sample. Each experiment was repeated at least three times, and the results represent the average of all

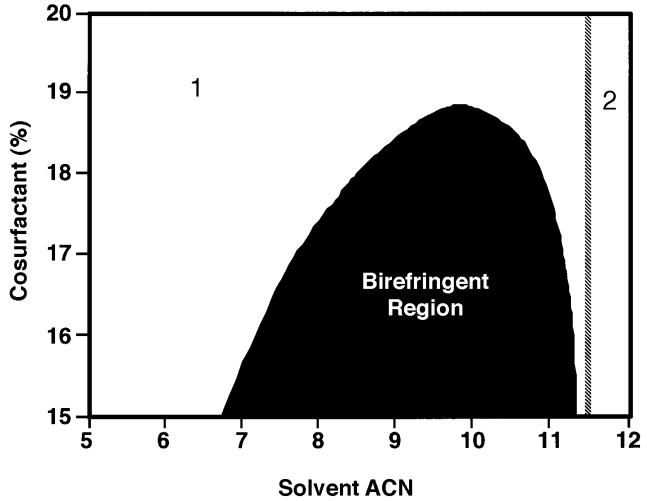


**FIG. 2.** Microemulsion structure vs. solvent alkane carbon number (ACN) and cosurfactant level, showing isotropic and optical birefringent regions. Also shown are single- (1) and two-phase (2) microemulsion regions.

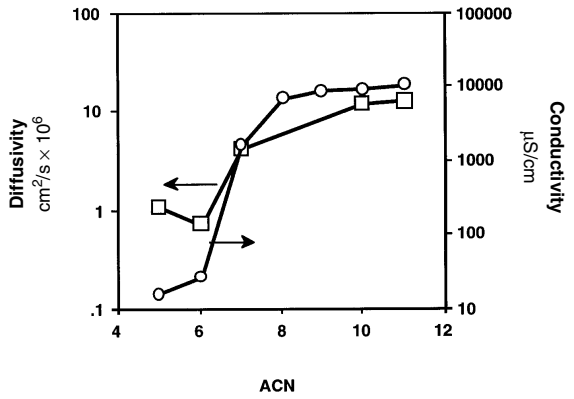


**FIG. 3.** Microemulsion conductivity and water diffusivity vs. solvent ACN at 20% cosurfactant. See Figure 2 for abbreviation.

three measurements. The microemulsion cleaning performance was compared to the performance of reference systems with identical compositions, in which the water was replaced by an equal volume of hydrocarbon solvent. The total weight of petroleum jelly used was always low relative to the solubilization capacity of the microemulsions. As a result, the solubilization data represent the solubilization rates of the microemulsions in question.

## RESULTS

The microemulsions contained a 1:1 (vol/vol) solvent/water ratio and were initially prepared with 5% surfactant and 15% cosurfactant. Subsequently, cosurfactant was added to the initial microemulsion samples to regulate liquid crystal content. The aqueous subphase contained 0.07 wt% added sodium chloride, and the electrolyte levels in the neat surfactant were determined as less than 70 ppm sulfate, 70 ppm chloride, and 80 ppm carbonate (all sodium salt forms). GC (Fig. 1) revealed that the alkylbenzene (surfactant precursor) consisted of a mixture of $C_{20}$ (74%), $C_{22}$ (22%), and $C_{24}$ (4%) ABS, with alkyl branching at the 2 (11.5%), 3 (9%), and higher (79.5%) positions. NMR data revealed nearly quantitative sulfonation (>99%) in the *para* position. No *ortho* or *meta* sulfonation was detected by NMR.

The microemulsion phase behavior vs. solvent ACN and cosurfactant level is shown in Figure 2. At 19% cosurfactant, single-phase microemulsions were obtained over a wide range of ACN values (5 to 11), whereas below 19 wt% cosurfactant, a thick birefringent region was observed in the single-phase microemulsion region (see Fig. 2).

An excess solvent phase was observed in equilibrium with the microemulsion phase at ACN values greater than $C_{11}$ [Winsor type I systems (1)]. The microemulsion structure was inferred from electrical conductivity and PGSE NMR data, as shown in Figure 3. For example, the data obtained at 20 wt% cosurfactant showed a gradual increase in electrical conductivity with increasing solvent ACN, indicating an increasingly water-continuous structure. This result is supported by PGSE results, showing that water self-diffusion coefficient increased with ACN (3). These results are consistent with an interpretation that increasing solvent ACN results in decreasing solvent/surfactant tail affinity leading to a transition from a solvent-continuous to water-continuous microemulsion structure.

Selected compositions within the birefringent region were characterized by small-angle X-ray scattering, which revealed

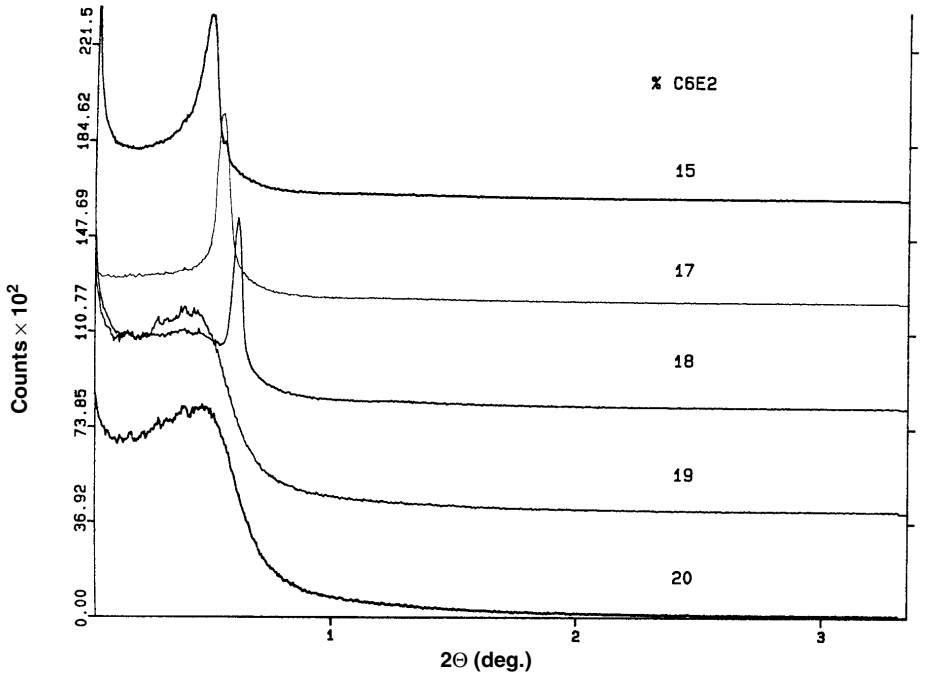


**FIG. 4.** Small-angle X-ray scattering patterns of microemulsion systems at 9.5 alkane carbon number vs. 2Θ for several cosurfactant levels. Cosurfactant is diethylene glycol monohexyl ether ($C_6E_2$).

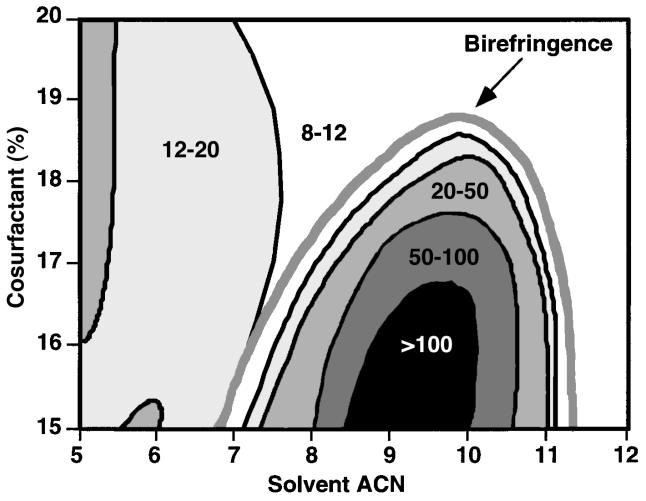


**FIG. 5.** Microemulsion system viscosity vs. ACN and percentage cosurfactant. Viscosity ranges (in centipoise) are shown in the graph. The thick grey line represents envelope of optical birefringence. See Figure 2 for abbreviations.

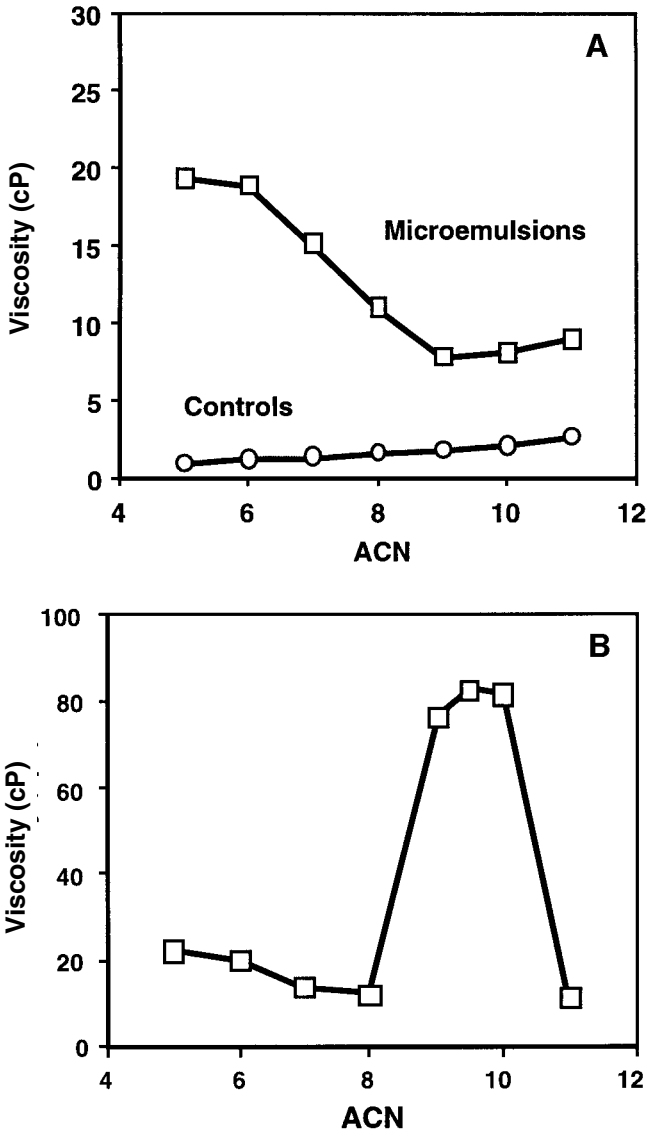


**FIG. 6.** Microemulsion and reference system viscosities vs. ACN: A, at 20% cosurfactant, and B, at 17% cosurfactant. See Figure 2 for abbreviation.

a lamellar liquid crystalline structure. Increasing cosurfactant concentrations resulted in a transition from liquid crystal to microemulsion structures (Fig. 4). The microemulsion system viscosity was mapped vs. ACN and cosurfactant level at a constant shear rate of 25 $s^{-1}$ (Figs. 5, 6). The viscosity was relatively low in the isotropic region of the diagram but became quite high in the dispersed liquid crystalline region. Furthermore, at 20% cosurfactant, the viscosity vs. ACN showed a minimum in the bicontinuous region. The liquid crystalline region showed shear-thinning behavior. In contrast, the single-phase microemulsions exhibited Newtonian rheology.

The relationship between liquid crystal content and viscosity was quantitated (Fig. 7) for a single ACN as a function of cosurfactant content. The liquid crystal content in the birefringent region clearly correlated with the viscosity in this series of compositions.

The large single-phase region in these systems may be interpreted by using qualitative models of surfactant cohesive free energy density (1). Low salt levels and large ($C_{20}$–$C_{24}$ alkylbenzene) surfactant hydrophobes give simultaneously high net surfactant head/water and tail/solvent affinity, resulting in a large single-phase microemulsion region that spans solvent-continuous to water-continuous structures. Increasing the salt concentrations resulted in a shift to a more solvent-continuous structure, while reducing salt concentration resulted in a more water-continuous structure. It was possible to obtain single-phase microemulsions within the $C_5$–$C_{12}$ ACN range at higher electrolyte levels by using a $C_{18}$ ABS. However, this resulted in reduced efficiency and did not give the wide single-phase region obtained with the $C_{20}$–$C_{24}$ systems.

Petroleum jelly cleaning was studied as a function of ACN at 17 and 20% cosurfactant levels to compare the performance of liquid crystal-containing systems with liquid crystal-free systems, while advancing from solvent-continuous to water-continuous microemulsion structures. The electrical conductivity and phase behavior of all microemulsions were monitored before and after the solubilization experiment, and no significant changes were detected as a result of the cleaning experiment.

Figure 8 shows the petroleum jelly cleaning of microemulsions and reference systems vs. solvent ACN and viscosity in the liquid crystal-free regime (20% cosurfactant). In general, cleaning performance was highest with the water-free reference systems. Here the reference systems were equivalent to the corresponding microemulsions, except the aqueous phase was replaced with an equal volume of solvent. As the solvent ACN was increased, the cleaning

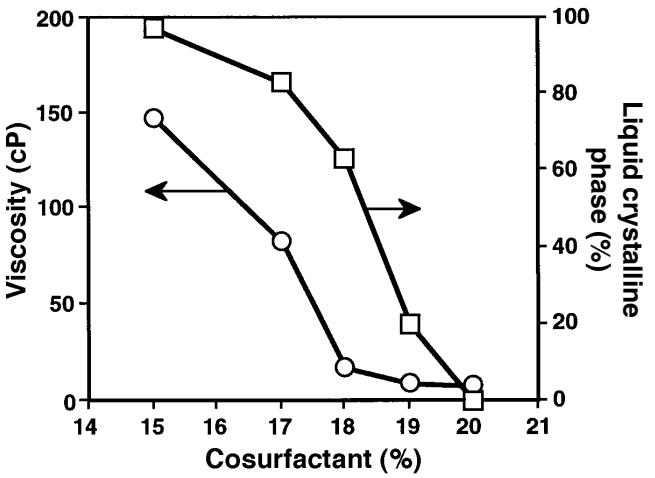


**FIG. 7.** Volume percentage liquid crystalline (LC) phase and viscosity vs. cosurfactant content at 9.5 alkane carbon number obtained after 1 h of centrifugation at 3450 rpm.

performance of both control and microemulsion systems dropped systematically. This drop may be attributed to the poorer solubilization power of the higher alkane solvents. Furthermore, cleaning of the microemulsion system approached but did not exceed cleaning of the reference system.

The effects of liquid crystals on cleaning performance were studied with a series of compositions that contained 17% cosurfactant. As ACN was increased, the compositions passed through a viscous liquid crystalline regime (Fig. 6). The cleaning performance of the viscous liquid crystal-containing compositions was much lower than the cleaning performance of the control systems or the liquid crystal-free microemulsion systems (Fig. 9). Interestingly, the relatively

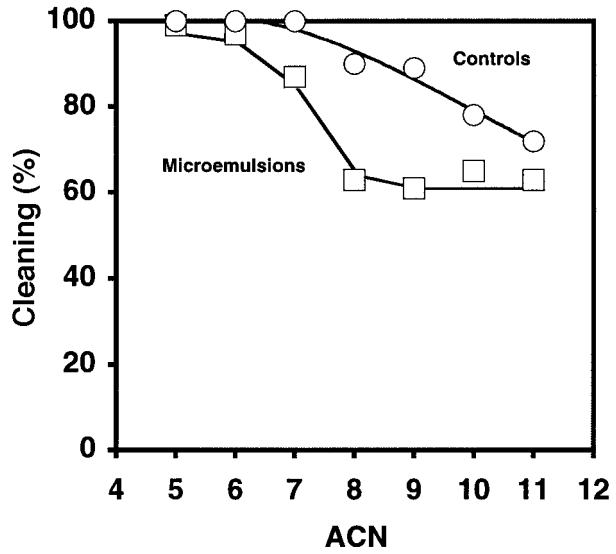


**FIG. 8.** Petroleum jelly solubilization performance of microemulsion systems and control systems vs. ACN at 20% cosurfactant. See Figure 2 for abbreviation.

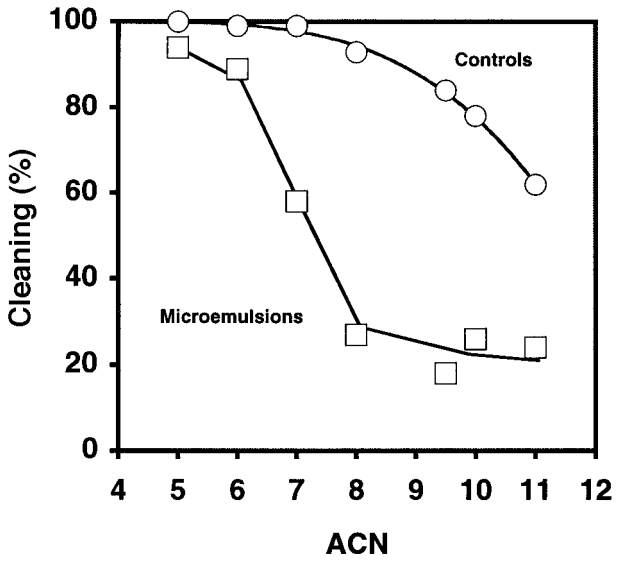


**FIG. 9.** Petroleum jelly solubilization performance of microemulsion systems and control systems vs. ACN at 17% cosurfactant. See Figure 2 for abbreviation.

poor cleaning performance at 17% cosurfactant extended somewhat outside the high-viscosity region.

In all aforementioned systems, microemulsion structural variations were accompanied by changes in solvent ACN and viscosity. All of these variations can influence cleaning performance. To isolate the effects of microemulsion structure (solvent- to water-continuous) on cleaning performance, a series of microemulsions was made with $C_8$ ACN, 20% cosurfactant, and various levels of sodium chloride to advance the structure from water-continuous to solvent-continuous. According to current interpretations, the electrolyte screens the ionic surfactant headgroups, inducing a water- to solvent-continuous transition with increasing electrolyte levels (1).

The normalized electrical conductivities and water diffusivities of these microemulsions are plotted in Figure 10.

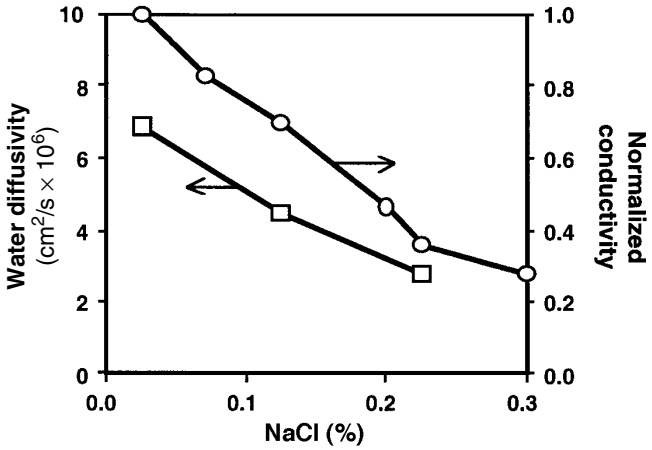


**FIG. 10.** Conductivity and water diffusivity of microemulsion systems vs. electrolyte level (aqueous) for $C_8$ alkane carbon number and 20% cosurfactant.

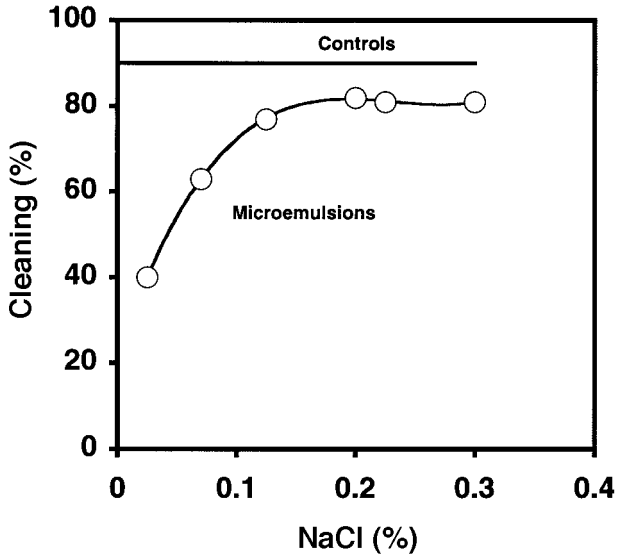


**FIG. 11.** Petroleum jelly solubilization vs. electrolyte level of microemulsion systems from Figure 10. Solubilization performance of control system ($C_8$ alkane carbon number, no water, no electrolyte added) is shown for comparison.

These data indicate that the microemulsions span substantially solvent-continuous to water-continuous structures. Furthermore, all of these microemulsions had viscosities (at 25 $s^{-1}$) between 11 and 12 centipoise. Thus, this series of microemulsions allows investigation of the effects of microemulsion structural variations, independent of variations in viscosity or solvent-phase composition.

In this series of compositions, maximum cleaning performance was obtained (Fig. 11) with microemulsions that exhibited nearly solvent-continuous structures (high electrolyte), and a sharp reduction in cleaning was noted for water-continuous structures (low electrolyte). Also, cleaning performance of the solvent-continuous microemulsions (approximately 80% removal) approached that of the water-free control systems at $C_8$ ACN (approximately 90% removal).

## DISCUSSION

These results show that the petroleum jelly solubilization performance of fluid bicontinuous microemulsions can approach that of water-free control systems. In particular, the optimal solubilization properties were obtained with substantially solvent-continuous and liquid crystal-free systems. The solubilization performance (at constant viscosity and solvent composition) increased systematically as the microemulsion structure was advanced from water-continuous to solvent-continuous structures *via* addition of electrolyte. In other experiments, system viscosity increases correlated with a marked reduction in cleaning performance.

The relative cleaning performance of solvent-continuous and water-continuous microemulsions may also depend on the nature of the cleaning process. In agitated systems, where convection is important, the performance of solvent-continuous and water-continuous structures may be quite similar, whereas in stagnant or mildly agitated systems (such as the one considered here), solubilization processes may be quite important, and one may expect the solvent- or bi-continuous structures to have greater cleaning performance than water-continuous systems. The effects of agitation and viscosity of these systems are being investigated, and results will be reported in a future publication.

## ACKNOWLEDGMENT

The authors acknowledge Virgil Turkelson for ion chromatography and carbonate analysis.

## REFERENCES

1. Bourrel, M., and R.S. Schechter, *Microemulsions and Related Systems: Formulation, Solvency and Physical Properties*, Marcel Dekker, New York, 1988, pp. 335–395.
2. Anonymous, Dow Launches Methyl Chloroform Substitutes, *Chemical Week*: 57 (October 12, 1994).
3. Lindman, B., and P. Stilbs, Molecular Diffusion in Microemulsions, in *Microemulsions: Structure and Dynamics*, edited by S.E. Friberg and P. Bothorel, CRC Press, Boca Raton, 1987, pp. 119–152.

[Received June 19, 1996; accepted March 17, 1997]